

LIMITATIONS AND SOLUTIONS OF BEAM SIZE MEASUREMENTS VIA INTERFEROMETRY AT ALBA

L. Torino, U. Iriso, ALBA-CELLS, Cerdanyola del Vallès, Spain

Abstract

The interferometry beamline at ALBA had several limitations which have been overcome over the past years until currently, beam size measurements are successfully performed using this technique. The main limitation has been related to vibrations in the light wavefront transportation along the beamline. Several counter-measures have been taken to overcome these limitations, related both to the software analysis and the mechanical setup, where the conventional double slit system is substituted by a double pinhole in order to obtain more light and a better interferogram. This report describes the current interferometry setup at ALBA, and show some results.

INTRODUCTION

After two years, interferometry is a reliable technique to measure the beam size at the ALBA storage ring. The diagnostic beamline Xanadu has been updated, analyzed and optimized to achieve good horizontal and vertical results using this technique [1].

The main parameters related with the beam size and the synchrotron radiation characteristics are listed in Table 1.

Table 1: ALBA Lattice Parameters

	x	y
β	0.299 m	25.08 m
Dispersion	0.04 m	0 m
Energy spread	0.001 01	
Emittance	4.6 nm	0.023 nm
Beam size	53.6 μm	23.9 μm

Several limitations due to the beamline layout have been overcome theoretically and practically. In this report the limitations and the solutions applied are described, and the results for both horizontal and vertical beam size measurements are presented.

MAIN LIMITATIONS

ALBA diagnostic beamline, Xanadu [2], takes the synchrotron radiation from a bending magnet. The light is selected by a photon shutter located at 1.684 m from the source point with an aperture of ± 3.2 mm in the horizontal plane and ± 5.5 mm in the vertical. After the shutter the light travels for roughly 7 m where a $\frac{1}{8}$ mirror extracts only the upper lobe of the visible radiation. The mirror is motorized and approaches the orbit plane (where the majority of the x-rays are concentrated) up to a distance of 7 mm, in order to maintain the heat load low. The radiation is extracted through a vacuum window ($\frac{1}{10}$) and transported outside the

tunnel in the experimental hutch through an optical path of 7 mirrors (Thorlabs, 4", $\frac{1}{10}$). The mirrors are located "in-air".

The full beamline had been updated in 2014. The improvements of the quality of the in-vacuum mirror, of the extraction window and of all the mirrors of the optical path, already gave the possibility to obtain some preliminary results, as presented in [3].

In any case, the layout of the beamline still presents two major limitations.

Diffraction

The footprint of the light reaching Xanadu is strongly affected from Fraunhofer diffraction [4]. The effect is due to the first horizontal cut of the light performed from the photon shutter (vertical strips), and the vertical one due to the extraction mirror (horizontal strips). An SRW [5] simulation of the footprint is shown in Fig. 1.

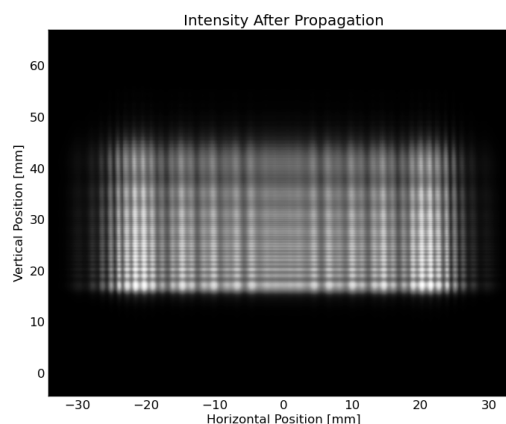


Figure 1: SRW simulation of the footprint reaching Xanadu diagnostic beamline.

When trying to perform interferometry, the use of long rectangular slits allows the selection of a large number of Fraunhofer fringes. The relative phase of these fringes is not necessarily the same and this provokes a modification in the interferogram that leads to a loss of contrast. A solution to this problem was found by using pinholes instead of slits, and adapting the theoretical formula describing the interferogram for this setup.

Vibrations

The second limitation is due to the fact that almost the whole beamline is in-air. This originates vibration in the optical components, which are sensible to air turbulence. This effect provokes changes in the interferogram characteristics and a rigid displacement of the centroid of the image.

Using an exposure time of 100 μs , and a fast acquisition camera working at 50 Hz, it was possible to reconstruct the spectrum of the vibration following the displacement of the interferogram centroid. The result of the FFT of the displacement in the horizontal (red) and vertical (blue) direction with respect to time is shown in Fig. 2: vertical vibration looks much more problematic and major peaks are present at 10 and 14 Hz.

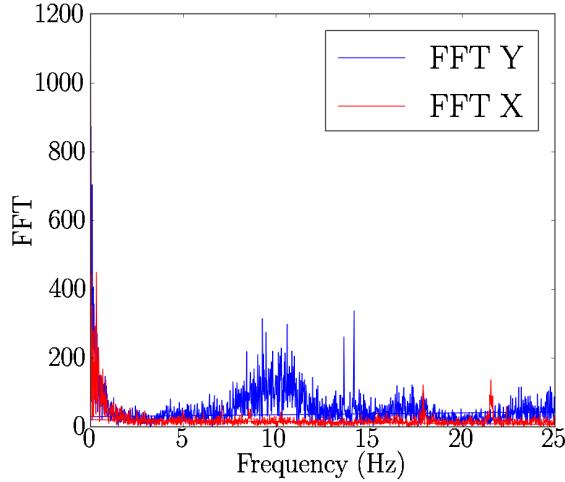


Figure 2: FFT of the displacement of the centroid of the interferogram in the horizontal (red) and vertical (blue) direction.

The problem can be reduced by lowering the exposure time of the CCD camera during the image acquisition. On the other hand, this decreases the quantity of light reaching the CCD sensor and the interferogram might be not clear enough the measure.

To overcome this problem, a dedicated algorithm was implemented to match more images together to improve the dynamic range of the measurement.

INTERFEROMETRY USING PINHOLES

The standard interferometry set-up in Accelerator physics is composed by a double slit system, as introduced by T. Mitsuhashi [1, 6]. Replacing the slits with pinholes forces to an adjustment of the formula, used by Mitsuhashi to fit the results.

The envelope of the interferogram is given by the Fourier transform of the shape of the aperture generating the interference [4, 7]. In the Mitsuhashi formula the envelope is parametrized by a $\text{sinc}(x)$, being this the Fourier transform of a rectangle. In the case of pinhole the resulting function is a Bessel function of the first type J_1 and the formula for the interferogram becomes:

$$I = I_0 \left\{ \frac{J_1 \left(\frac{2\pi ax}{\lambda f} \right)}{\left(\frac{2\pi ax}{\lambda f} \right)} \right\}^2 \times \left\{ 1 + V \cos \left(\frac{2\pi Dx}{\lambda f} \right) \right\}, \quad (1)$$

where I_0 is the intensity of the interferogram, a is half diameter of the pinhole, f is the focal distance of the optical

system used, λ is the radiation wavelength, V is the visibility ($\approx \frac{I_{Max} - I_{Min}}{I_{Max} + I_{Min}}$), and D is the distance between the pinhole centers. Obtaining V from the fit, and using the distance between the source point and the pinholes, L , the beam size is computed as:

$$\sigma = \frac{\lambda L}{\pi D} \sqrt{\frac{1}{2} \ln \frac{1}{V}}. \quad (2)$$

The use of pinholes instead of slits makes the alignment easier, and allows to select more uniform zones of the footprint. As a consequence, less Fraunhofer fringes are selected, and the contrast of the interferometry results improves.

For this reason the ALBA experimental set-up is composed by a double pinhole system. The diameter of the pinholes is 3 mm (good results were obtained with pinholes up to ≈ 6 mm), and the separation between them is 16 mm (or larger if using larger pinholes).

CCD EXPOSURE TIME

An intuitive and convenient way to reduce the effect due to the beamline vibrations and the air turbulences is the reduction of the exposure time of the CCD camera, which reduces the number of oscillations during the image acquisition (as well as the superposition of artificially shifted interferograms).

This behavior is well summarized in the plot in Fig. 3. The plot shows the results for the horizontal and vertical beam size, taken in the same conditions at different exposure times.

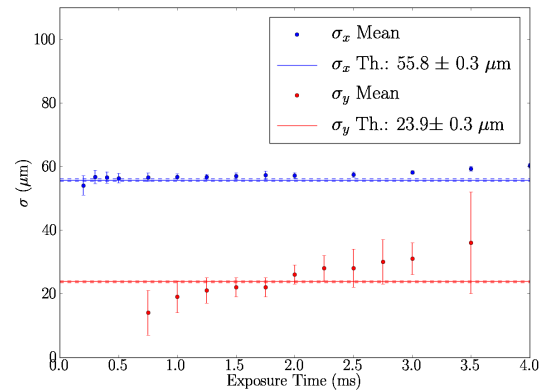


Figure 3: Horizontal (blue) and vertical beam size as a function of the exposure time. Solid lines represent the expected value. Error bars corresponds to statistical measurement fluctuations.

In general, for low exposure time, the measured beam size is smaller with respect to the expected, and the statistical error bar is quite big since the fit is not able to properly reconstruct the image. At high exposure time the measured beam size is larger with respect to the theoretical one, since several shifted interferogram are summed up during the long acquisition time, affecting the contrast. The effect is much

more evident for the vertical measurements with respect to the horizontal, this is mainly due to two reasons. First the horizontal beam size is almost double of the vertical, therefore the expected visibility for the horizontal measurements is smaller and does not require such a high contrast for the images. Second, the vibration of the optical path due to the Xanadu layout are much stronger in the vertical direction (as shown in Fig. 2).

The reasonable choice for the exposure time is to be chosen among the ones in the plateau in Fig. 3, where the image distortion due to vibrations is minimized. For this reason, the usual exposure time set for beam size measurements is 1.5 ms.

HORIZONTAL BEAM SIZE MEASURE

An example of interferogram for horizontal beam size measurements is shown in Fig. 4. To obtain the final result, the projection of the central part (10 rows) of the interferogram is fitted using Eq. (1). The resulting visibility is then plugged in Eq. (2) and the beam size is obtained.

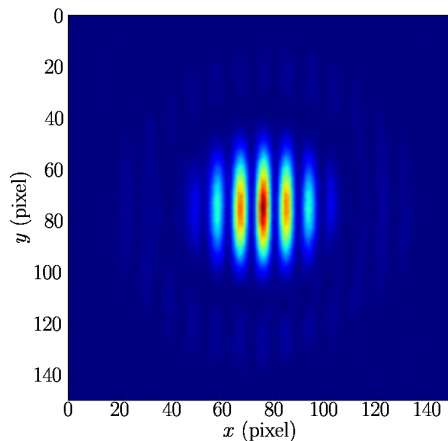


Figure 4: Horizontal Interferogram.

An alternative way to measure the beam size with the interferometer technique is to perform a scan of the distance between the pinholes, D . This parameter is indeed the Fourier conjugate of the beam size: inverting Eq. (2) one obtains:

$$V = e^{-2\pi \frac{\sigma^2 D^2}{\lambda^2 L^2}}. \quad (3)$$

Considering the visibility as a function of D the expected result is a Gaussian. Fitting the results letting the beam size as a free parameter, it is possible to obtain σ .

Depth of Field

It is interesting to study with this method the effects of the Depth of Field due to the photon shutter aperture (± 1.9 mrad). Because this aperture, the light reaching Xanadu is creating a blurring of the image due to the curvature of the trajectory. The bending radius of the magnet producing the radiation is 7.05 m, that leads to blurring of

$\pm 13 \mu\text{m}$. This incoherent effect can be observed when measuring the horizontal beam size using the pinholes distance scan.

Figure 5 shows the visibility as a function of the distance between the pinholes. The data (red dots) are fitted with a Gaussian that take into account the effect of the Depth of Field:

$$V = e^{-2\pi \frac{\sigma^2 D^2}{\lambda^2 L^2} + \sigma_{DoF}^2}. \quad (4)$$

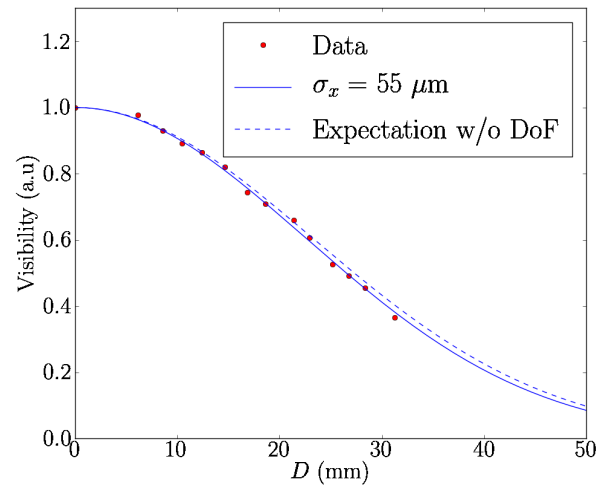


Figure 5: Visibility as a function of the distance between pinholes.

The solid line is the result of the fit using Eq. (4) and fixing $\sigma_{DoF} = 26 \mu\text{m}$. The dashed line is the theoretical curve (Eq. (3)) without the effects of the depth of field, and using as σ the result of the previous fit. The fit is providing the expected results for the horizontal beam size. This shows that the depth of field must be taken into account when performing this measurements.

Vertical beam size measures are not affected by this effect since the light is not coming from the orbit plane.

VERTICAL BEAM SIZE MEASURE

The limitations of Xanadu beamline were mostly affecting the vertical beam size measure, but thanks to the adjustments it is now possible to achieve reliable results.

Coupling Scan

To prove that the vertical interferometry beam size measurements are effective, scans of the beam coupling are performed. Varying the current in the skew magnets, the beam coupling varies as well as the vertical beam size.

Vertical beam size measurements are performed for several couplings and the results are compared to the one obtained with the x-rays pinhole. The pinhole and the Xanadu beamline take the synchrotron radiation from the two consecutive dipoles, at different locations inside the magnet. During normal operations, as well as during the coupling

scan, the vertical and the horizontal beam size differs one from the other of a few μm .

As an example, in Fig. 6, the vertical beam size of the pinhole (in blue) and of the interferometry (in red) are plotted as a function of the beam coupling.

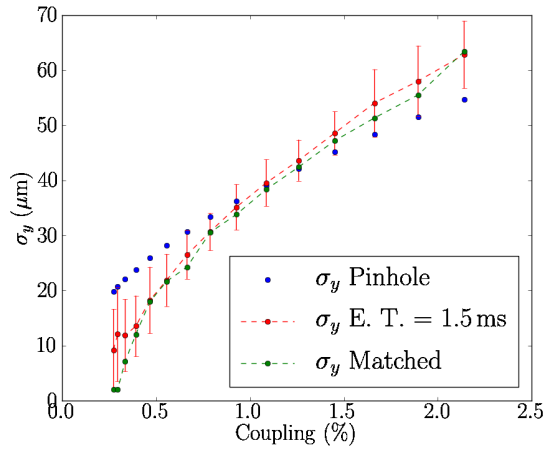


Figure 6: Vertical beam size measured with the pinhole (blue), with the interferometry (red), and interferometry with the application of the matching algorithm, as a function of the coupling.

The interferometry measurements follow nicely the one of the pinhole when the coupling is varying. Several coupling scans were performed and in all the cases the two curves intercept each other around a coupling of 1.2%. The ALBA operation coupling is around 0.5% and, as expected, the interferometry beam size is smaller with respect the pinhole one. After the 1.2% coupling the interferometry measurements are larger with respect to the one of the pinhole.

Results of these tests prove the effectiveness of the interferometry measurements performed at ALBA.

Matching Algorithm

In order to keep the exposure time as low as possible, an algorithm to superimpose several interferograms was implemented in Python.

The experimental set-up is the same that the one described in previous case. The exposure time was set to 100 μs , the minimum given by the CCD, and data were acquired for 1 minute at 50 Hz to obtain 3000 interferograms.

The raw interferogram at 100 μs of exposure time is presented in Fig. 9a. Data are very noisy and it is not possible to obtain a good result by fitting.

The algorithm takes the first interferogram acquired as reference, computes the correlations between this and the others, and shifts them of the resulting quantity. Figure 7 presents the horizontal and vertical distances the interferograms needed to be shifted in order to be matched with the reference.

The images are shifted until the interferograms can all be superimposed with the proper centroid match.

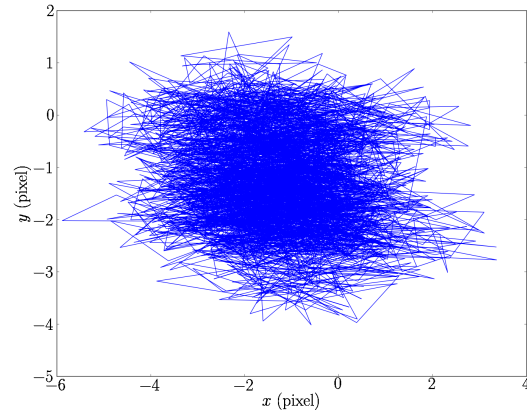


Figure 7: Distribution of the shifts to be applied to match the images.

The data analysis is done considering the projection of the central columns of the interferogram. Figure 8 shows the 3000 projections without (blue) and with (red) the application of the matching algorithm.

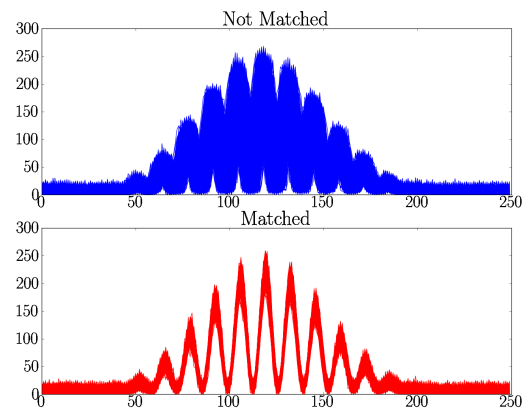


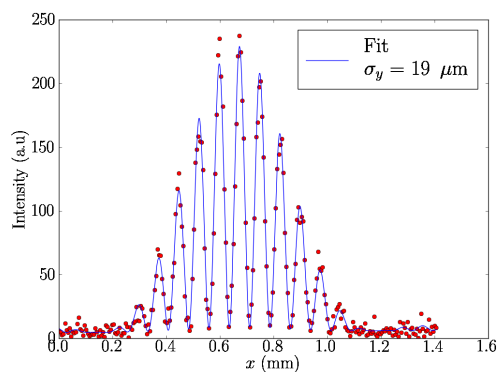
Figure 8: Plot of the 3000 projections without (blue) and with (red) the application of the matching algorithm.

It is clear that summing the projections without the application of the algorithm leads to a loss of contrast and a consequent reduction of the visibility, while for the projections of the matched images the effect is strongly reduced.

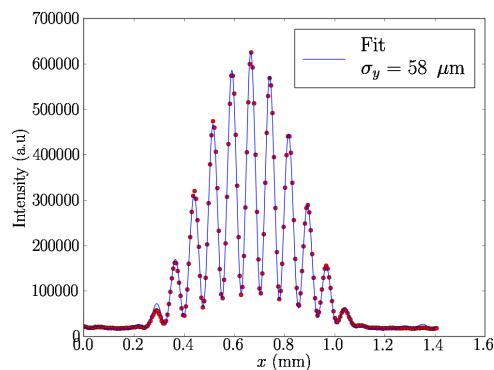
The interferogram as sum of the unmatched images is presented in Fig. 9b. The result of the fit provides a larger beam size because of the loss of contrast. The result obtained by applying the algorithm is shown in Fig. 9c. The matching algorithm improves both dynamic range and contrast of the final interferogram.

In order to prove the algorithm performance a coupling scan was carried out and the matching algorithm was applied to reconstruct the interferograms at different coupling.

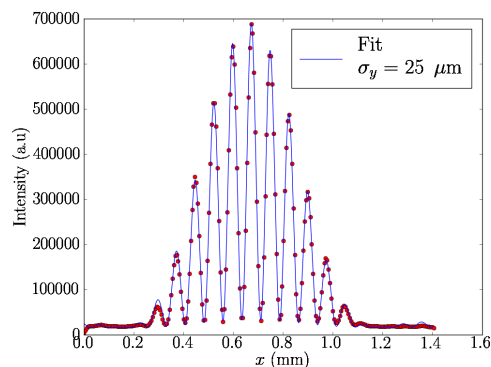
Green dots in Fig. 6 present the beam size using the matching algorithm. Also in this case the obtained values are consistent.



(a) Single acquisition.



(b) Not matched.



(c) Matched.

Figure 9: Fit of the interferograms for different acquisition methods.

CONCLUSION

After a period of commissioning the beam size measurements using interferometry are finally fully reliable at ALBA.

The use of pinholes instead of slits reduced the loss of contrast due to the Fraunhofer diffraction. Measurements showed that it is possible to balance the loss of contrast due to vibrations and the low dynamic range of the camera, by reducing the exposure time of the image acquisition accordingly.

It was possible to study the effect of the incoherent depth of field on the horizontal beam size measurements analyzing the visibility distribution as a function of the pinholes separation. On the other hand the efficiency of vertical beam size measurements was proved performing coupling scans and verifying that interferometry was able to reproduce the result of the pinhole. Finally an algorithm was developed in order to match images displaced by vibration acquired at very low exposure times. Also in this case coupling scans were performed to prove the goodness of the algorithm.

ACKNOWLEDGMENT

This work owns a lot to J. Nicolás for the enlightening discussions on optics. Thanks also to S. Blanch for the development of the fast acquisition software of the CCD camera and all the technical staff of ALBA.

This project is funded by the European Union within the oPAC network under contract PITN-GA-2011-289485.

REFERENCES

- [1] T. Mitsuhashi, "SR Monitor – Special topics", BIW2012, Newport, April 2012, TUAP02 (2012)
- [2] U. Iriso et al., "Diagnostics during the ALBA SR commissioning", DIPAC-2011, Hamburg, May 2011, TUOA02 (2011)
- [3] L. Torino et al., "Beam Size Measurements using Synchrotron Radiation Interferometry at ALBA", IBIC-2014, Monterey, September 2014, TUPF23 (2014)
- [4] M. Born and E. Wolf, *Principles of Optics, 7th edition*, (Cambridge University press, 2006)
- [5] O. Chubar et al., "Accurate and Efficient Computation of Synchrotron Radiation in the Near Field Region", EPAC-1998, Stockholm, June 1998, 1177 (1998)
- [6] T. Mitsuhashi, "Measurement of small transverse beam size using interferometry", DIPAC'2001, Grenoble, May 2001, IT06 (2001)
- [7] A. Glindemann, "Introduction to Spatial Interferometry" https://www.eso.org/sci/facilities/paranal/telescopes/vlti/tuto/tutorial_spatial_interferometry.pdf